Tectonophysics 454 (2008) 36–43

Contents lists available at ScienceDirect

Tectonophysics

journal homepage: www.elsevier.com/locate/tecto

A forward test of the Decelerating–Accelerating Seismic Strain model to western south and central America

B.C. Papazachos [a], Ch.A. Papaioannou [b], E.M. Scordilis [a,*], C.B. Papazachos [a], G.F. Karakaisis [a]

[a] Department of Geophysics, School of Geology, Aristotle University, GR54124, Thessaloniki, Greece
[b] Institute of Engineering Seismology and Earthquake Engineering (ITSAK), Foinikas, GR55102 Thessaloniki, Greece

ARTICLE INFO

Article history:
Received 30 May 2007
Received in revised form 26 February 2008
Accepted 20 March 2008
Available online 7 April 2008

Keywords:
Decelerating seismic strain
Accelerating seismic strain
Earthquake prediction
South America

ABSTRACT

Global observations show that strong mainshocks are preceded by decelerating preshocks which occur in the focal (seismogenic) region of the ensuing mainshock and by accelerating preshocks which occur in a broader (critical) region of the mainshock. Predictive properties of these preshocks have been expressed by empirical relations supported by theory and form the Decelerating–Accelerating Seismic Strain (D–AS) model. A respective algorithm has been developed which is used to identify the critical and seismogenic region and estimate (predict) the corresponding ensuing mainshock. In the present work a forward test of this model is performed by attempting intermediate-term prediction of future big ($M \geq 7.7$) mainshocks along the western coast of south and central America. Three regions of decelerating shocks and three corresponding regions of accelerating shocks have been identified. The parameters (origin time, magnitude, epicenter coordinates) as well as their uncertainties have been estimated (predicted) for the corresponding probably ensuing three mainshocks. This forward test allows an objective evaluation of the model's ability for an intermediate-term prediction of strong shallow mainshocks.

1. Introduction

Precursory seismic excitation in a broad region accompanied by decreasing seismicity in the focal region of strong mainshocks has been observed some decades ago and was called "doughnut pattern" by Mogi (1969). This general concept, which expresses qualitatively a behavior of precursory seismic activity, has been supported by quantitative investigation of precursory seismic activity. It led to the important conclusion that precursory seismic activity in the broad region is accelerating and in a narrower region is decelerating with the time to the mainshock.

Accelerating seismicity concerns the accelerating generation of intermediate magnitude preshocks with the time to the mainshock and has been extensively investigated (Tocher, 1959; Raleigh et al., 1982; Sykes and Jaumé, 1990; Knopoff et al., 1996; Brehm and Braile, 1999; Papazachos and Papazachos, 2001; Robinson, 2000; Tzanis et al., 2000; Papazachos et al., 2005b; Mignan, 2006, among many others). On the basis of a damage mechanics model, Bufe and Varnes (1993) proposed the following relation for the time variation of the cumulative Benioff strain, $S(t)$ (in Joule$^{1/2}$), released by accelerating preshocks at the time, t:

$$S(t) = A + B(t_c - t)^m \quad (1)$$

where t_c is the origin time of the mainshock and A, B and m are parameters determined by the available data with $m < 1$. Bowman et al. (1998) suggested the minimization of a curvature parameter, C, which is defined as the ratio of the root-mean-square error of the power–law (relation 1) to the corresponding linear-fit error and used this parameter to identify regions of accelerating preshocks. Accelerating precursory seismicity has been interpreted in terms of the critical point dynamics (Sornette and Sornette, 1990; Sornette and Sammis, 1995; Rundle et al., 2000; 2003) or by the Stress Accumulation Model (Bowman and King, 2001; King and Bowman, 2003).

Decrease of the frequency of small preshocks in the focal region in respect to the background frequency, called "seismic quiescence", has been also observed by many researchers (Wyss and Habermann, 1988; Jaumé, 1992; Bufe et al., 1994; Zöller et al., 2002, among others) and has been attributed to stress relaxation due to aseismic sliding (Wyss et al., 1981; Kato et al., 1997). Precursory transient seismic excitation followed by continuous decrease of the seismic strain, called "decelerating seismic strain", has been observed before many mainshocks and its variation with the time to the mainshock is also fitted by a power–law (relation 1) with $m > 1$ (Papazachos et al., 2005a, b). Decelerating seismic strain is attributed to static stress shadow (Papazachos et al., 2006) predicted by the Stress Accumulation Model (Bowman and King, 2001; King and Bowman, 2003).

Papazachos et al. (2006) by taking into consideration the relative published information on decelerating and accelerating seismic strain, and using recent (since 1980) reliable data on such sequences of already occurred strong ($M \geq 6.4$) mainshocks in a variety of seismotectonic

* Corresponding author.
E-mail addresses: kpapaza@geo.auth.gr (B.C. Papazachos), chpapai@itsak.gr (C.A. Papaioannou), manolis@geo.auth.gr (E.M. Scordilis), kpapaza@geo.auth.gr (C.B. Papazachos), karakais@geo.auth.gr (G.F. Karakaisis).

0040-1951/$ – see front matter © 2008 Elsevier B.V. All rights reserved.
doi:10.1016/j.tecto.2008.03.012

regimes, developed the "Decelerating–Accelerating Seismic Strain" (D–AS) model and a corresponding algorithm for intermediate term prediction of strong (M>6.0) shallow (h≤100 km) mainshocks. This model is expressed by empirical relations with predictive properties and has been tested by its application on preshock sequences of seven complete samples of 46 strong (M=6.3–8.3) mainshocks which occurred in various seismotectonic regimes (W. Mediterranean, Aegean, Anatolia, Central Asia, Japan, California, S. America). However, this backward procedure is not enough and forward testing, by attempting predictions of future mainshocks, is necessary for a more objective evaluation of the predictive ability of the model. Predictive properties of the accelerating pattern have been already applied (in 2002) for the successful intermediate term prediction of the 8.1.2006 large (M=6.8) earthquake which occurred in the southwestern part of the Aegean (Papazachos et al., 2007). This is encouraging for forward tests of the model like that attempted in the present work.

The purpose of the present work is to apply the D–AS model on data for shocks (preshocks) which occurred up to 1 October 2007 in the western part of south and central America in order to estimate (predict) the basic parameters (origin time, magnitude, epicenter coordinates) of big (M≥7.7) shallow (h≤100 km) mainshocks in this area. We limited our investigation to such big mainshocks because smaller shocks in this region are usually associated shocks (postshocks, aftershocks) which cannot be predicted by this method. This restriction in the mainshock magnitude and the restriction in the focal depth of the mainshock and of preshocks (h≤100 km) result from a backward test of the method in south and central west America.

The D–AS model has been developed by data of earthquakes which occurred in the Mediterranean, California, central Asia, south and central west America and Japan. For the first three areas forward tests of the model have been already attempted. In these three areas, however, no broad subduction zones and no big (M>8.0) earthquakes occur while such zones and earthquakes occur in the last two areas. This is the main reason for which such test is performed in the present paper for south and central west America. We are now preparing a forward test for Japan too.

Papazachos et al. (1997) have developed the "regional time and magnitude predictable model" (R-TM), which can also contribute to intermediate term earthquake prediction. The basic relations of this model are:

$$\log T = 0.19M_{\min} + 0.33M_p + q \tag{2}$$

$$M_f = 0.73M_{\min} - 0.28M_p + m \tag{3}$$

where, T is the interevent time between the mainshocks of a region, $M_{\min}$ is the minimum mainshock magnitude, M_p is the magnitude of the previous mainshock, M_f is the magnitude of the following mainshock and q, m are parameters which are calculated by the available data of the region. This is a time-dependent model since the time of the following mainshock in a region depends on the magnitude, M_p, of the previous mainshock and can be used for intermediate term prediction. Thus, in the present work, relation (3) is used to calculate an additional value for the magnitude of the predicted mainshock.

The investigated area is formed of two long seismic zones. The first one extends along the western coast of south America, has an almost north–south direction (45° S–5° N, 65° W–84° W) and is a result of convergence of the south American lithosphere with the Nazca lithospheric plate. The second one is a narrow seismic zone which has a SE–NW direction and is defined by the geographic points (5° N, 65° W), (5° N, 84° W), (16° N, 106° W), (24° N, 106° W). This seismic zone is a result of convergence of the north American and Caribbean lithospheric plates with the Cocos lithospheric plate. Fig. 1 shows the epicentres of the shallow (h≤100 km) earthquakes which occurred during the period 1900–2007 in the investigated area (along the western coast of south and central America) and have moment magnitudes M≥7.7.

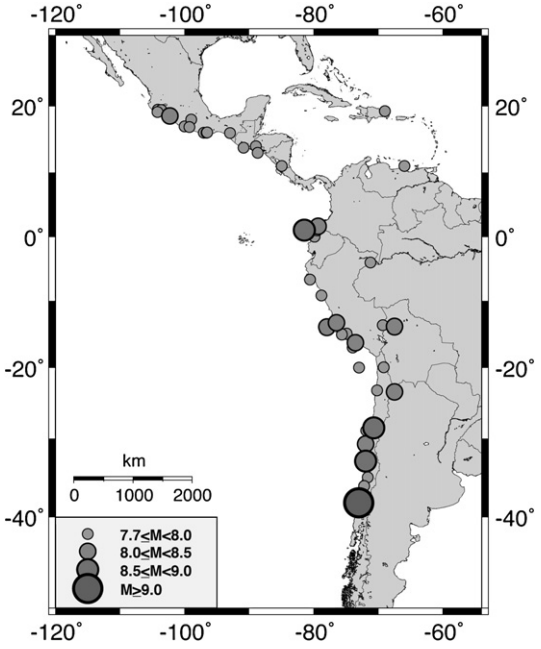

Fig. 1. Distribution of epicenters of the shallow (h≤100 km) earthquakes with M≥7.7 which occurred along the west coast of south and central America during the period 1900–2007.

2. The Decelerating–Accelerating Seismic Strain (D–AS) Model

The D–AS model is formed of relations with predictive properties which can be separated in three categories. The first category includes relation (1) and other relations, which concern accelerating preshocks and are used for the estimation (prediction) of the origin time and the magnitude of the ensuing mainshock. The second category of relations includes also relation (1) and other relations which concern decelerating preshocks and are used to estimate (predict) another value for the origin time of the mainshock and another value for its magnitude. The relations of the third category are based on properties of both accelerating and decelerating shocks (preshocks) and are used to estimate (predict) the epicenter coordinates of the ensuing mainshock. All these relations are based on global observations but most of them have been derived theoretically and/or interpreted physically (Papazachos et al., 2006).

2.1. Accelerating preshocks

An accelerating preshock sequence follows relation (1) with m<1 and the relations:

$$\log R = 0.42M - 0.30 \log s_a + 1.25, \qquad \sigma = 0.15 \tag{4}$$

$$\log(t_c - t_{sa}) = 4.60 - 0.57 \log s_a, \qquad \sigma = 0.10 \tag{5}$$

$$M = M_{13} + 0.60, \qquad \sigma = 0.20 \tag{6}$$

$$\log(t_c - t_a) = 3.11 - 0.36 \log s_a \tag{7}$$

where R (in km) is the radius of the circular (critical) region, s_a (in Joule$^{1/2}$/yr 10^4 km^2) is the rate of the long-term seismic strain, t_{sa} (in yr) is the start time of the accelerating sequence, t_c is the origin time of the mainshock, M is the magnitude of the mainshock, M_{13} is the mean magnitude of the three largest preshocks and t_a is the mean origin time of the accelerating preshocks.

A "quality index", q_a, is defined by the relation:

$$q_a = \frac{P_a}{mC} \tag{8}$$

where P_a is the arithmetic mean of the probabilities that each obtained solution (M, R, t_{sa}, t_c) conforms with the global relations (1, 4, 5, 6) assuming that the deviation of each parameter follows a Gaussian distribution (Papazachos et al., 2002). Application of this procedure on a large sample of accelerating preshock sequences (Papazachos et al., 2005b) resulted in the following cut-off values:

$$C \leq 0.60, P_a \geq 0.45, m \leq 0.35, q_a \geq 3.0 \quad (9)$$

Worldwide observations show that the mean value of m is 0.30, which is in agreement with theoretical considerations (Rundle et al., 1996; Ben-Zion et al., 1999) and for these reasons this value of m is adopted in the present work. The magnitude, $M_{\min}$, of the smallest preshock of an accelerating preshock sequence for which relations (9) hold and q_a has its largest value is given (Papazachos et al., 2005b) by the relation:

$$M_{\min} = 0.46M + 1.91 \quad (10)$$

where M is the magnitude of the mainshock. Thus, for M=6.0, 7.0 and 8.0 the $M_{\min}$ is 4.7, 5.1 and 5.6, respectively.

The geographic point, Q, for which relations (9) hold and the quality index, q_a, has its largest value for a particular accelerating preshock sequence is considered as the geometrical center of the critical region, that is, the center of the circle with radius, R, given by relation (4). In addition to Q there are two other distinct geographic points (V_q, P_q) which are defined by the distribution of the epicenters of accelerating preshocks and are useful for studying time dependent seismicity. V_q is the geographic mean (mean latitude, mean longitude) of the epicenters of the shocks of an accelerating preshock sequence. P_q is the geographic point from where the density (number of epicenters per unit area) of accelerating preshocks decays with the distance according to a power–law and is called physical center of the accelerating sequence (Karakaisis et al., 2007).

2.2. Decelerating preshocks

For a decelerating preshock sequence a power–law (relation 1 with $m>1$) and the following relations hold:

$$\log a = 0.23M - 0.14\log s_d + 1.40, \qquad \sigma = 0.15 \quad (11)$$

$$\log(t_c - t_{sd}) = 2.95 - 0.31\log s_d, \qquad \sigma = 0.12 \quad (12)$$

where a (in km) is the radius of the circular (seismogenic) region where the epicenters of decelerating preshocks are located, M is the magnitude of the mainshock, t_{sd} (in yr) is the start time of the decelerating preshock sequence, and s_d (in Joule$^{1/2}$/yr 10^4 km^2) is the long-term seismic strain-rate (long-term seismicity) of the seismogenic region (Papazachos et al., 2006).

A quality index, q_d, has been also defined for each decelerating preshock sequence by the relation:

$$q_d = \frac{P_d m}{C} \quad (13)$$

where P_d is the mean value of the probabilities that each one of the quantities (a, M, t_{sd}, t_c) of an obtained solution fits the global relations (11, 12), assuming that the deviation of each parameter follows a Gaussian distribution. The following cut-off values have been calculated by the use of global data (Papazachos et al., 2006):

$$C \leq 0.60, 2.5 \leq m \leq 3.5, P_d \geq 0.45, q_d \geq 3.0 \quad (14)$$

From a large number of globally occurred decelerating preshock sequences, an average value equal to 3.0 has been derived for m and this value is adopted in the present work. Attempts for retrospective "predictions" with different values of m did not lead to any decrease of uncertainties. The minimum magnitude, $M_{\min}$, of a decelerating preshock sequence for which the best (optimum) solution is obtained, is given by the relation:

$$M_{\min} = 0.29M + 2.35 \quad (15)$$

where M is the magnitude of the mainshock. Thus, for M=6.0, 7.0 and 8.0 the $M_{\min}$ is equal to 4.1, 4.4 and 4.7, respectively.

The geographic point, F, for which relations (14) are fulfilled and where q_d has its largest value is considered as the geometrical center of decelerating preshocks, that is, the center of the circle which includes the epicenters of decelerating preshocks and has radius, a (in km), given by relation (11). There are also two other geographic points (V_f, P_f), which are defined by the distribution of the epicenters of the decelerating preshocks. V_f is the geographic mean of the epicenters of decelerating preshocks. P_f is the physical center of the decelerating preshocks from where the density of the epicenters of these preshocks decays with the distance according to a power–law (Karakaisis et al., 2007).

2.3. Relations for locating the mainshock epicenter

The estimation (prediction) of the geographic coordinates of the epicenter of an ensuing mainshock is based on the locations of the six distinct geographic points (F, V_f, P_f, Q, V_q, P_q), which are defined by the space distribution of the preshocks. This estimation is also based on the values of the quality indexes (q_{de}, q_{ae}) in the mainshock epicenter, E, in respect to their values (q_{df}, q_{aq}) in the geometrical centers (F, Q) of already occurred mainshocks (Papazachos et al., 2006).

The six distinct geographic points are separated in two groups. The first group is formed of the three distinct geographic points (F, V_f, P_f), which are at relatively short distances from the mainshock epicenter and their geographic mean (mean latitude, mean longitude) is a point, D, the distance of which from the mainshock epicenter, E, is:

$$(\mathrm{ED}) = 110 \pm 50 \text{ km} \quad (16)$$

The second group is also formed of the three distinct geographic points (Q, V_qV$_q$, P$_q$) which are at relatively large distances from the mainshock epicenter and their geographic mean, A, is in a distance from the mainshock epicenter, E, which is given by the relations:

$$\begin{array}{ll} (\mathrm{AE}) = 150 \pm 40 \text{ km}, & (\mathrm{DA}) \leq 230 \text{ km} \\ (\mathrm{AE}) = (\mathrm{AD}) \pm 100 \text{ km}, & (\mathrm{DA}) > 230 \text{ km} \end{array} \quad (17)$$

Relations (16, 17) form the first two constraints for the mainshock epicenter.

From investigation of a large number of preshock sequences it comes out that the mainshock epicenters have a tendency to delineate along the line DA and lie symmetrically with respect to this line. Thus, by considering as positive the distances from the line DA of the epicenters which are in one side of this line and as negative these distances of the epicenters which are in the other side, it is found that the mean, x, of all distances is equal to zero with a standard deviation 80 km. That is:

$$x = 0 \pm 80 \text{ km} \quad (18)$$

This is the third constraint for the mainshock epicenter.

Measures of precursory decelerating and accelerating seismic strain have smaller values in the mainshock epicenter than in the corresponding geometrical centers (e.g. $q_{de} < q_{df}$, $q_{ae} < q_{aq}$). This has been expressed by the following relation:

$$\frac{q_{de} + q_{ae}}{q_{df} + q_{aq}} = 0.45 \pm 0.13 \quad (19)$$

which forms a fourth constraint for the location of the mainshock epicenter.

There is a point, L, of the grid where the probability for a random generation of a shock is highest. The distance of this point from the mainshock epicenter is given by the relation:

$$(\mathrm{EL}) = 110 \pm 70 \text{ km} \tag{20}$$

which forms the fifth constraint for the location of the mainshock epicenter.

Therefore, the D–AS model defines quantitatively the space, time and magnitude distributions of preshocks with empirical relations which are supported by physical models and can be used, in principle, to predict the origin time, t_c, the magnitude, M, and the epicenter coordinates of ensuing mainshocks.

3. The data

A complete and homogeneous earthquake catalogue covering the broader area of study and extending over a wide time period is required for the present work. The main data sources that were used for this purpose are the bulletins of the International Seismological Centre (ISC, 2007) and the National Earthquake Information Centre (NEIC, 2007) of the USGS, as well as the online CMT catalogue of Harvard (2007).

The compiled catalogue (Papaioannou et al., 2007) concerns a broad area bounded by the coordinates 50° S–30° N, 120° W–54° W and covers the time interval 1900–September 2007. Magnitudes in the above data sources are given in several scales (M_s, m_b, M_L, M_{JMA}, M_w). To ensure the homogeneity of the catalogue with respect to the magnitude, the moment magnitude scale was selected as the most reliable one. All other magnitudes were transformed into the moment magnitude scale, M_w ($=M$), by appropriate formulae (Scordilis, 2005, 2006). We applied these formulae for conversions to moment magnitude because these are based on a larger sample of data than previously proposed conversion formulae (e.g. Utsu, 2002). The reliability of this conversion is also evidenced by successful backward tests of the model based on such magnitude conversions. The finally adopted magnitude for each earthquake is either the original moment magnitude (published by Harvard or USGS) or the equivalent moment magnitude estimated as the weighted mean of the converted magnitude values, by weighting of each participating magnitude with the inverse standard deviation of the respective relation applied. The errors in the magnitudes of the catalogue are up to 0.3 and in the locations up to 30 km, which are satisfactory for the purpose of the present work. The finally compiled catalogue (Papaioannou et al., 2007) includes information on 50,956 earthquakes with equivalent moment magnitudes $3.5 \le M \le 9.6$, focal depths up to ~670 km and covers the period 1900–September 2007.

This catalogue is complete for magnitude ranges that depend on the region and on the time periods that were tested. Three complete samples of data are required in this study: a) one sample of shocks to calculate the long-term strain rates (s_a, s_d) needed in relations (4, 5, 7, 11 and 12), b) a second sample of shocks (decelerating preshocks) to calculate the decelerating with time Benioff strain, and c) a third sample of shocks (accelerating preshocks) to calculate the accelerating with time Benioff strain.

From previous studies in several areas globally (Mediterranean, California, Himalayas) it has been shown that for reliable estimation of long-term strain rates (s_a, s_d), time periods which include shocks with $M \ge 5.2$ are the proper ones. Consequently, the minimum magnitude $M=5.2$ is selected in the present case for defining the corresponding time period to calculate the long-term strain rates. The completeness of the data was checked for several sub-regions, time periods and cut-off magnitudes using both the frequency–magnitude and cumulative frequency–magnitude relation. It has been finally found (Fig. 2) that the catalogue

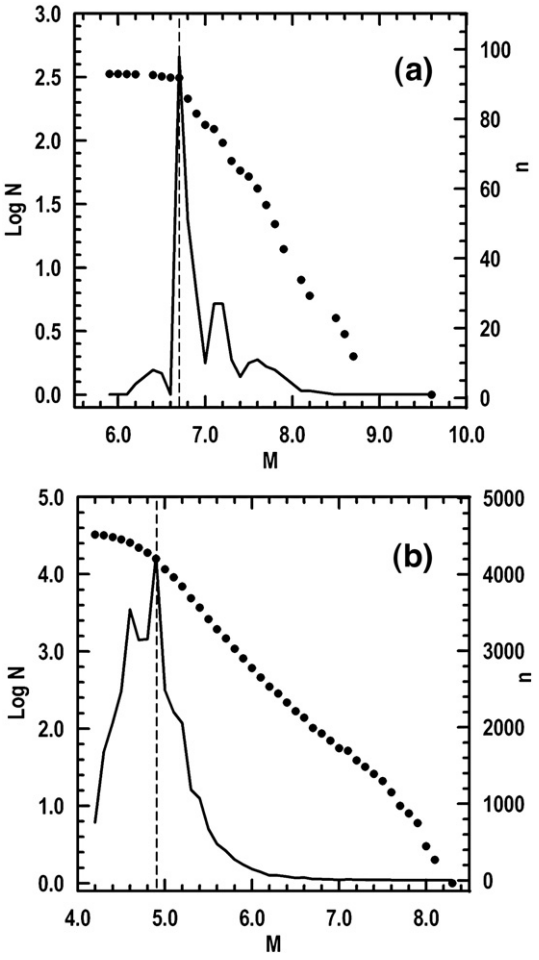

Fig. 2. Frequency (right axis) and cumulative frequency (left axis)–magnitude distributions for the time periods: 1900–1964 (a), 1965–2007 (b) for the broader area of the west coast of central and south America.

is complete for the following periods and corresponding magnitudes:

$$\begin{array}{ll} 1900-1964 & M \ge 6.7 \\ 1965-2007 & M \ge 4.9 \end{array} \tag{21}$$

From relations (21) it comes out that the data-set for the period 1965–2007 can be used for the estimation of the long-term seismicity rates (s_a, s_d), since all earthquakes that occurred in the tested area during this time period with $M \ge 5.2$ are included.

The D–AS model has been tested for shallow shocks (preshocks, mainshocks). It has been also observed that for shocks in big subduction zones the data of shocks with focal depths up to 100 km contribute positively to the improvement (increase) of the quality indexes (q_d, q_a). For this reason shocks with $h \le 100$ km are considered in the present work.

Declustering for removing aftershocks has no important effect on the results because duration of aftershocks is of the order of weeks to months while preshock sequences last from years to decades. For this reason the data used in the present work have not been declustered.

4. Procedure followed

In order to identify probable seismogenic regions where decelerating preshocks currently occur and corresponding critical regions where accelerating preshocks occur and estimate the mainshock parameters (origin time, magnitude, epicenter coordinates), a three-step procedure is followed. The critical and seismogenic regions are

Table 1
Parameters of the circular region of decelerating seismic strain (first line) and of the circular region of accelerating seismic strain (second line)

	t_c	F/Q	M	a/R	C	q	M_{min}	n	t_s	logs
1	2012.2	−22.8, −73.2	8.4	331	0.27	8.8	4.7	34	1996	5.59
	2009.5	−26.5, −72.2	8.6	2045	0.47	6.1	6.0	197	1967	5.22
2	2009.7	1.0, −76.9	8.6	416	0.28	10.5	4.7	162	1991	5.42
	2010.3	−1.0, −77.0	8.7	2236	0.39	7.2	6.0	233	1965	5.19
3	2011.7	19.5, −99.0	8.0	307	0.27	10.8	4.6	107	1993	5.42
	2011.1	18.0, −98.0	8.5	1875	0.43	7.5	5.7	427	1964	5.13

F/Q is the geometrical center of the region, t_c (in years) is the estimated origin time for the expected mainshock, M is its magnitude, a/R (in km) is the radius of the region, C is the curvature parameter, q is the quality index, M_{min} is the magnitude of the smallest shock (preshock), n is the number of these shocks, t_s is the start year of the sequence and s (in Joule$^{1/2}$/yr 10^4 km^2) is the long-term strain rate in each region.

considered as circular although the algorithm can also treat elliptical regions. The reason for this is that the results are very similar for circular and elliptical regions and calculations for circles are much faster.

During the first step the whole search area of western south America and western central America has been separated by a grid of points (e.g. 0.2° NS, 0.2° EW). Each grid point is considered as the geometrical center of a circular seismogenic region where decelerating preshocks occur and the radius, a in (km), varies in a range defined by relation (11) and its uncertainties, with a certain step (e.g., 5 km). The strain rate, s_d (in Joule$^{1/2}$/yr 10^{4}km^2), is calculated for each circle by using the sum of the square root of seismic energy (Benioff strain), released by shocks with $M \geq 5.2$ which occurred in the circle during the period 1.1.1965–1.10.2007, divided by the product of the area of the circle (in 10^{4}km^2) and the time duration (~43 yr). This is done for a range of mainshock magnitudes between 7.7 and 9.0 with a certain step (e.g. 0.2) and of t_{sd} in a certain step (e.g. 1 yr). The minimum searched value of mainshock magnitude (M=7.7) was chosen because backward tests of the D–AS model in South America (Papazachos et al., 2006) show that smaller earthquakes in this area are, usually, associated shocks (preshocks, aftershocks, postshocks). So, shocks with $M<7.7$ cannot be considered as mainshocks in this area and cannot be predicted by this model. An initial preliminary value is estimated for t_c on the basis of the identification time of the preshock sequence (Papazachos et al., 2006). The Benioff strain (square root of seismic energy) is calculated by information on all shocks (decelerating preshocks) with M_{min} given by relation (15) that have epicenters within each circle and occurred since t_{sd}. For each circle (each a), each M and each t_{sd} the parameters A, B of relation (1) with m=3.0, the curvature parameter C, the probability P_d and the quality index q_d (relation (13)) which fulfill relations (14) are calculated.

It has been observed that the values of q_d are spatially clustered in three groups. The geographic point of each group for which q_d has the maximum value is considered as the geographic center, F, of the seismogenic region and the corresponding solution (t_c, $F(\varphi,\lambda)$, M, a, C, q_d, M_{min}, n, t_{sd}, logs_d) is considered as the best solution for this group. This optimization procedure is repeated for several assumed values of t_c. The value of M which corresponds to the best solution is considered as one of the two values estimated by the D–AS method for the magnitude of the expected mainshock. A value of the origin time, t_c, of the expected mainshock is also estimated in this first step of the procedure, by the application of relation (12) and the use of t_{sd} and s_d of the obtained (by optimization) best solution.

In the second step of this procedure the same broad area of the western south and central America has been searched and three corresponding circular critical regions, where accelerating shocks (preshocks) currently occur, were identified. The geometrical center, Q, of each critical region and the best solution (t_c, $Q(\varphi,\lambda)$, M, R, C, q_a, M_{min}, n, t_{sa}, logs_a) were defined by considering the largest value of q_a. The corresponding magnitude to this best solution is considered as a second value of the magnitude, M, of the expected mainshock. A third value for this magnitude is calculated by relation (3). Two additional values for the origin time, t_c, are calculated by relations (5) and (7) and the use of t_a, t_{sa} and s_a of the best solution for the accelerating strain.

In the third step of this procedure the geographic coordinates of the epicenter, $E(\varphi, \lambda)$, of the expected mainshock have been estimated on the basis of relations (16–20). That is, these relations have been tested for each point of the grid and five corresponding probabilities are calculated for each of these points, by assuming a Gaussian distribution for the observed deviations. The average of the five probabilities is considered as the representative value of each geographic point and the point with the highest representative probability has been considered as the mainshock epicenter.

5. Model uncertainties

Application of the above described procedure on preshock sequences of a large number of globally already occurred mainshocks indicates model uncertainties equal to ±2.5 years for the origin time, ±0.4 for the moment magnitude and up to 150 km for the epicenter of a mainshock, with a high probability (~90%) for the occurrence of a mainshock within all three windows. However, errors are also due to false alarms, as it is indicated by tests on synthetic catalogues (Papazachos et al., 2002, 2005a, 2006). This probability for false alarms of the D–AS model has been estimated by the following procedure (Papazachos et al., 2006). The original earthquake catalogue for a selected region (Aegean area) was initially declustered by applying the Poisson distribution for the time of occurrence of shocks and the Gutenberg–Richter relation for their magnitude distribution in each seismic zone of this area. The random (Poisson) distribution of shocks in space and time was estimated and adopted to the declustered catalogue. Finally, aftershocks following the known time and space patterns were added to evaluate the final synthetic catalogue. Such tests on a large number of synthetic catalogues of the D–AS model (false presence of joint decelerating–accelerating patterns) indicate a low probability (~10%).

Therefore, the probability for the occurrence of a mainshock predicted by the D–AS model is about 80%, if we take into consideration the probability (~90%) for the defined model errors (based on *a posteriori* predictions) and the probability (~90%) found through tests for false alarms on synthetic catalogues. This probability is compared in each case with the probability for random occurrence of an expected mainshock, which is calculated by applying the Gutenberg–Richter recurrence relation for the distribution of the magnitudes of a complete sample of shocks and assuming a standard Poisson distribution for the time variation of these shocks.

6. Results

Table 1 gives the estimated parameters (t_c, $F(\varphi,\lambda)$, M, a, C, q_d, M_{min}, n, t_{sd}, logs_d) of the best solution (in the first line for each of the three cases) which come from the decelerating seismic strain, where n is the

Table 2
The estimated origin time, t_c, epicenter coordinates, $E(\varphi,\lambda)$, and magnitude, M, for each of the three probably ensuing mainshocks in the western south and central America

	t_c	$E(\varphi,\lambda)$	M	P_r
1	2010.9	22.60 S, 71.30 W	8.2	0.08
2	2010.6	0.10 S, 77.50 W	8.5	0.14
3	2011.4	18.00 N, 100.00 W	8.0	0.07

Model uncertainties are: ±2.5 years for the origin time, ≤150 km for the epicenter, ±0.4 for the magnitude and focal depth $h \leq 100$ km for each expected mainshock, with an about 80% probability. The probability, P_r, for random occurrence of a mainshock with magnitude M±0.4 during a time period of 5 years in each predicted circular region is given in the last column of the table.

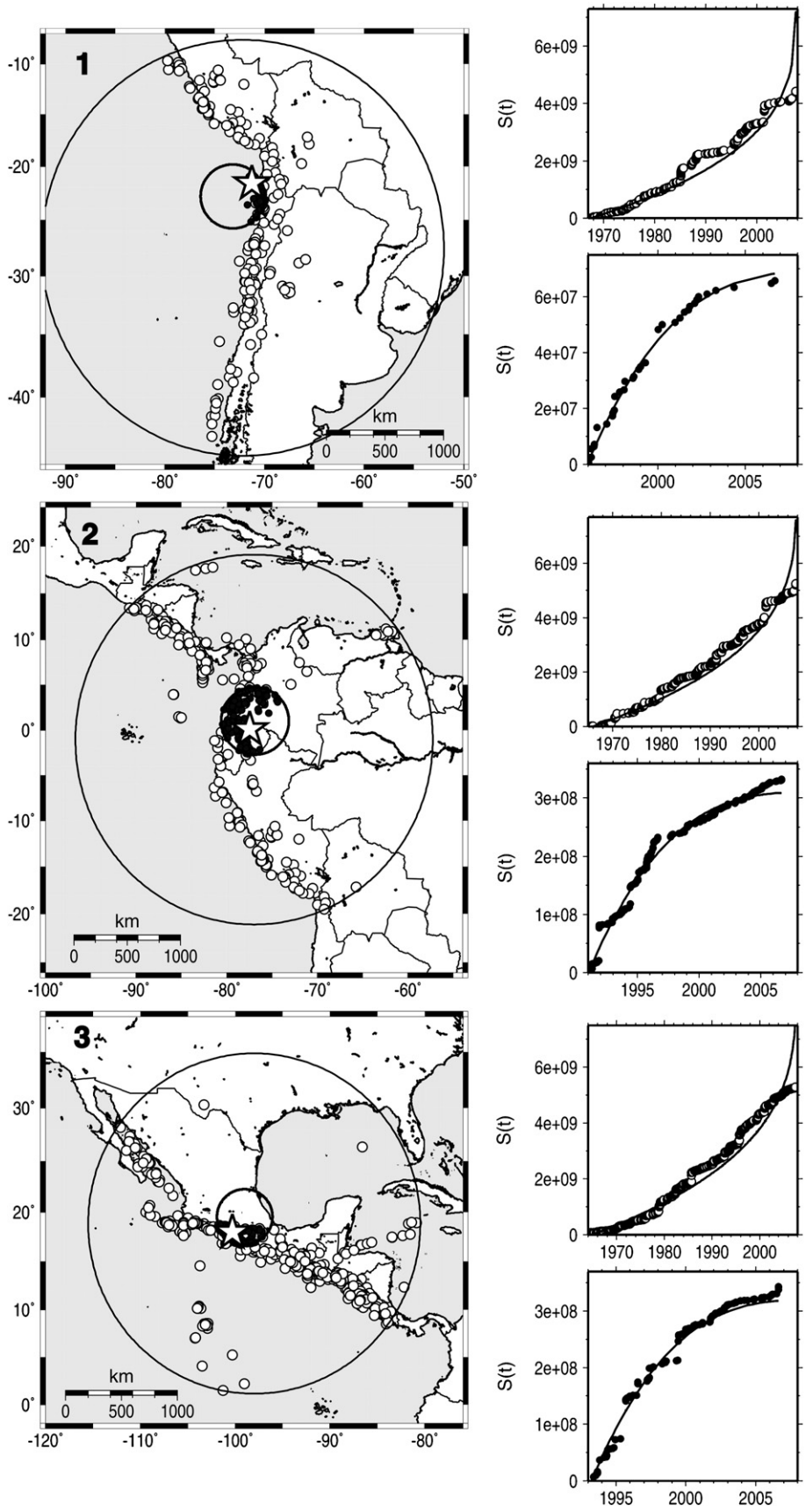

Fig. 3. Information on the decelerating–accelerating strain in the western part of south America (1, 2) and of central America (3). Dots are epicenters of decelerating shocks (preshocks), which are included in the smaller circular (seismogenic) region and small open circles are epicenters of accelerating shocks (preshocks), which are included in the larger circular (critical) region. The stars denote the predicted epicenters of the expected mainshocks. The time variation of the decelerating and accelerating Benioff strain, S(t), are shown at the right part of each case. The best-fit lines of the time variation of the Benioff strain which follow a power–law relation (1), are also shown.

number of decelerating shocks (preshocks). In the same table the estimated parameters (t_c, $Q(\varphi,\lambda)$, M, R, C, q_a, M_{min}, n, t_{sa}, $\log s_a$) of the best solution (in the second line for the three cases) for accelerating seismic strain are also included.

The finally estimated (predicted) values for the origin time, t_c, moment magnitude, M, and epicenter coordinates, $E(\varphi,\lambda)$, for each one of the three probably ensuing mainshocks are listed in Table 2. The errors in these estimated parameters are ±2.5 years for the origin time, ±0.4 for the magnitude and ≤150 km for the epicenter of the expected mainshock, with a probability of about 80%, which expresses the model uncertainties and takes also into account false alarms based on test on synthetic but realistic catalogues.

This probability must be compared with the probabilities for random occurrence of earthquakes in each one of the three predicted regions as well as in the broader area of western south and central America examined in the present work. These random probabilities have been estimated by the use of the complete data with $M \geq 5.2$ for the period 1965–2007 and the application of the Gutenberg–Richter relation for the magnitude distribution and of the Poisson distribution for the time of shocks. These probabilities, P_r, have been calculated for $M \geq 7.7$ and period of 5 years, which is the time window and are listed in Table 2, while this probability for the whole searched area of western south America is 0.50 and of western central America is 0.38.

Fig. 3 shows, on corresponding maps, the epicenters of the decelerating shocks (dots), the epicenters of the accelerating shocks (small open circles), the circular seismogenic regions (circles which include epicenters of decelerating shocks) and the circular critical regions (larger circles which include epicenters of accelerating shocks). The numbers (1, 2 and 3) correspond to the three cases and the code numbers of Tables 1, 2. The corresponding time variations of the cumulative Benioff strain for accelerating and decelerating shocks are also shown, together with the best-fit lines, which fit the data according to the power–law relation (1) with $m=0.3$ for accelerating strain and $m=3.0$ for decelerating strain.

7. Discussion

In the present work all scientific information is given for an objective backward evaluation of the predictions made in this paper, after the expiration of the estimated time windows (e.g. 2014). This information concerns the predicted parameters (epicenter coordinates, origin time, magnitude) and their uncertainties, the probability for the occurrence of the earthquakes in the defined space, time and magnitude windows, as well as the probability for random occurrence of each earthquake in these windows. An accurate definition of the broad area which has been searched for the identification of the D–AS pattern is also made. Thus, the occurrence or non-occurrence of such big mainshocks in regions of the broad area where no such pattern has been identified is also considered in the evaluation. However, for the application of a scientifically valid procedure of evaluation the following additional information is also necessary.

The present paper deals with predictions of big mainshocks ($M \geq 7.7$). The D–AS model has (in principle) the ability to predict only the largest earthquake (mainshock) of a clustered in space and time seismic sequence, which also includes other (associated) shocks (preshocks, postshocks, which occur in a network of neighboring faults). Associated shocks cannot be predicted by this procedure because their preshock region and preshock time cannot be identified as they are part of the preshock region and time of the mainshock. In some (rare) cases associated shocks are comparable in size with the mainshock and their epicenter, origin time and magnitude can also be within the predicted space, time and magnitude windows.

Thus, the generation of at least one earthquake with: focal depth $h \leq 100$ km, observed epicenter within a circle of radius 150 km and center the predicted epicenter, observed magnitude equal to the predicted magnitude ±0.4 and origin time the predicted origin time ±2.5 years, will be considered as a success. The non generation of a predicted earthquake within these space, time and magnitude windows will be considered as failure. As a failure will be also considered the generation of an earthquake with $M \geq 7.7$ and $h \leq 100$ km in any part of the investigated broad area of south and central western America, and outside of the three predicted space windows but within the time windows.

The probability for occurrence of each one mainshock in its predicted time, space and magnitude windows is 80%, while the corresponding probabilities for random occurrence are much smaller (less than 0.20). The probability for random occurrence of a mainshock with $M \geq 7.7$ in the broader searched area of south and central western America within a time period equal to the predicting time (5 years) has been found to be 0.50 and 0.38, respectively.

The main handicap of the model applied in the present work is that when the generation of more than one mainshocks is physically prepared in a network of neighboring faults the critical regions are mixed (contaminated) and only the largest of these mainshocks can be predicted. The model uncertainty in the epicenter location in such cases can be more than 150 km (up to 250 km).

Thus, the information given in the present work allows the objective evaluation of the prediction attempted in this paper. We can, for example, consider as quantitative measure of the evaluation a success ratio defined as the ratio of the sum of the number of success cases to the sum of the number of all cases (success and failure). In case of full failure (none of the three predicted earthquakes occur within the predicted windows) the success ratio takes a zero value. In case of full success (all three predicted mainshocks occur and no mainshock with $M \geq 7.7$ occurs in the broader searched area) this ratio is equal to unit.

Finally, it must be pointed out that prediction of individual earthquakes for social purposes is a hard and probably long process and that the present work was realized in the framework of such efforts.

Acknowledgements

The authors are grateful to both anonymous reviewers and the editor whose thoughtful comments and suggestions helped us to clarify certain issues and improve this paper significantly. Thanks are also due to Wessel and Smith (1995) for freely distributing the GMT software that was used to produce the maps of the present study.

References

Ben-Zion, Y., Dahmen, K., Lyakhovsky, V., Ertas, D., Agnon, A., 1999. Self-driven mode switching of earthquake activity on a fault system. Earth Planet. Sci. Lett. 172, 11–21.
Bowman, D.D., Quillon, G., Sammis, C.G., Sornette, A., Sornette, D., 1998. An observational test of the critical earthquake concept. J. Geophys. Res. 103, 24359–24372.
Bowman, D.D., King, G.C., 2001. Accelerating seismicity and stress accumulation before large earthquake. Geophys. Res. Lett. 28, 4039–4042.
Brehm, D.J., Braile, L.W., 1999. Intermediate-term earthquake prediction using the modified time-to-failure method in southern California. Bull. Seismol. Soc. Am. 89, 275–293.
Bufe, C.G., Varnes, D.J., 1993. Predictive modeling of seismic cycle of the Great San Francisco Bay Region. J. Geophys. Res. 98, 9871–9883.
Bufe, C.D., Nishenko, S.P., Varnes, D.J., 1994. Seismicity trends and potential for large earthquakes in Alaska–Aleutian region. Pure Appl. Geophys. 142, 83–99.
HRVD (Harvard Seismology), 2007. CMT catalogue. URL: http://www.seismology.harvard.edu/CMTsearch.html.
ISC (International Seismological Centre), 2007. On-line Bulletin. Internat. Seis. Cent., Thatcham, United Kingdom. URL: http://www.isc.ac.uk/Bull.
Jaumé, S.C., 1992. Moment release rate variations during the seismic circle in the Alaska–Aleutians subduction zone. Proceed. of Wadati Conference on Great Subduction Earthquakes, University of Alaska, pp. 123–128.
Karakaisis, G.F., Papazachos, C.B., Panagiotopoulos, D.G., Scordilis, E.M., Papazachos, B.C., 2007. Space distribution of preshocks. Boll. Geof. Teor. Appl. 48, 371–383.
Kato, N., Ohtake, M., Hirasawa, T., 1997. Possible mechanism of precursory seismic quiescence: Regional stress relaxation due to preseismic sliding. Pure Appl. Geophys. 150, 249–267.
King, G.C., Bowman, D.D., 2003. The evolution of regional seismicity between large earthquakes. J. Geophys. Res. 108. doi:10.1029/2001JB000783.
Knopoff, L., Levshina, T., Keilis-Borok, V.J., Mattoni, C., 1996. Increase long-range intermediate-magnitude earthquake activity prior to strong earthquakes in California. J. Geophys. Res. 101, 5779–5796.

Mignan, A., 2006. The Stress Acumulation Model. Phd. Thesis, Inst. de Physique du Globe de Paris, 219 pp.
Mogi, K., 1969. Some features of the recent seismic activity in and near Japan II. Activity before and after great earthquakes. Bull. Earthq. Res. Inst. Univ. Tokyo 47, 395–417.
NEIC (National Earthquake Information Center), 2007. Earthquake Hazards Program. URL: http://neic.usgs.gov/neis/epic/index.html.
Papaioannou, Ch.A., Scordilis, E.M., Papazachos, C.B., Karakaisis, G.F., Papazachos, B.C., 2007. A catalogue of earthquakes in central and south America for the period 1900–2007. Publ. Geoph. Laboratory. University of Thessaloniki.
Papazachos, B.C., Papadimitriou, E.E., Karakaisis, G.F., Panagiotopoulos, D.G., 1997. Long-term earthquake prediction in the circum-Pacific convergent belt. Pure Appl. Geophys. 149, 173–217.
Papazachos, B.C., Karakaisis, G.F., Papazachos, C.B., Scordilis, E.M., 2007. Evaluation of the results for an intermediate term prediction of the 8 January 2006 M_w=6.9 Cythera earthquake in southwestern Aegean. Bull. Seismol. Soc. Am. 97 (1B), 347–352.
Papazachos, C.B., Papazachos, B.C., 2001. Precursory accelerating Benioff strain in the Aegean area. Ann. Geofis. 144, 461–474.
Papazachos, C.B., Karakaisis, G.F., Savvaidis, A.S., Papazachos, B.C., 2002. Accelerating seismic crustal deformation in the southern Aegean area. Bull. Seismol. Soc. Am. 92, 570–580.
Papazachos, C.B., Scordilis, E.M., Karakaisis, G.F., Papazachos, B.C., 2005a. Decelerating preshock seismic deformation in fault regions during critical periods. Bull. Geol. Soc. Greece 36, 1–9.
Papazachos, C.B., Karakaisis, G.F., Scordilis, E.M., Papazachos, B.C., 2005b. Global observational properties of the critical earthquake model. Bull. Seismol. Soc. Am. 95, 1841–1855.
Papazachos, C.B., Karakaisis, G.F., Scordilis, E.M., Papazachos, B.C., 2006. New observational information on the precursory accelerating and decelerating strain energy release. Tectonophysics 423, 83–96.
Raleigh, C.B., Sieh, K., Sykes, L.R., Anderson, D.L., 1982. Forecasting southern California earthquakes. Science 217, 1097–1104.
Robinson, R., 2000. A test of the precursory accelerating moment release model on some recent New Zealand earthquakes. Geophys. J. Int. 140, 568–576.
Rundle, J.B., Klein, W., Gross, S., 1996. Dynamics of a traveling density wave model for earthquakes. Phys. Rev. Lett. 76, 4285–4288.
Rundle, J.B., Klein, W., Turcotte, D.L., Malamud, B.D., 2000. Precursory seismic activation and critical point phenomena. Pure Appl. Geophys. 157, 2165–2182.
Rundle, J.B., Turcotte, D.L., Shcherbakov, R., Klein, W., Sammis, C., 2003. Statistical physics approach to understanding the multiscale dynamics of earthquake fault systems. Rev. Geophys. 41 (4), 1019. doi:10.1029/2003RG000135.
Scordilis, E.M., 2005. Globally valid relations converting M_s, m_b and M_{JMA} to M_w, at Meeting on earthquake monitoring and seismic hazard mitigation in Balkan countries. NATO ARW, Borovetz, Bulgaria, 11–17 September 2005, pp. 158–161.
Scordilis, E.M., 2006. Empirical global relations converting M_s and m_b to moment magnitude. J. Seismol. 10, 225–236.
Sornette, A., Sornette, D., 1990. Earthquake rupture as a critical point. Consequences for telluric precursors. Tectonophysics 179, 327–334.
Sornette, D., Sammis, C.G., 1995. Complex critical exponents from renormalization group theory of earthquakes: implications for earthquake predictions. J. Phys. I. 5, 607–619.
Sykes, L.R., Jaumé, S., 1990. Seismic activity on neighbouring faults as a long term precursor to large earthquakes in the San Francisco Bay area. Nature 348, 595–599.
Tocher, D., 1959. Seismic history of the San Francisco bay region. Calif. Div. Mines Spec. Rep. 57, 39–48.
Tzanis, A., Vallianatos, F., Makropoulos, K., 2000. Seismic and electrical precursors to the 17-1-1983, M=7 Kefallinia earthquake, Greece, signatures of a SOC system. Phys. Chem. Earth, Part A Solid Earth Geod. 25, 281–287.
Utsu, T., 2002. Relationships between magnitude scales. Int. Handb. Earthq. Eng. Seismol. 81, 733–746.
Wessel, P., Smith, W., 1995. New version of the generic mapping tools. EOS 76–329.
Wyss, M., Klein, F., Johnston, A.C., 1981. Precursors of the Kalapana M=7.2 earthquake. J. Geophys. Res. 86, 3881–3900.
Wyss, M., Habermann, R.E., 1988. Precursory seismic quiescence. Pure Appl. Geophys. 126, 319–332.
Zöller, G., Hainzl, S., Kurths, J., Zschau, J., 2002. A systematic test on precursory seismic quiescence in Armenia. Nat. Hazards 26, 245–263.